Res. Chem. Intermed., Vol. 22, No. 9, pp. 839-854 (1996)

REDUCTION OF PYRACYLENE BY ALKALI METALS: MECHANISM AND FORMATION OF AGGREGATES

GIL ZILBER[+], VLADIMIR ROZENSHTEIN[+], ARI AYALON[+], HAIM LEVANON[+*], MORDECAI RABINOVITZ[+*], LAWRENCE T. SCOTT[#], HOPE B. WARREN[§], GABY PERSY[§] and JAKOB WIRZ[§]

[+]*Institute of Chemistry, The Hebrew University of Jerusalem, Jerusalem 91904, Israel*
[#]*Merkert Chemistry Center, Boston College, Chestnut Hill, MA, 02167-3860 USA*
[§]*Institut für Physikalische Chemie der Universitat Basel, Klingelbergstr. 80 CH-4056 Basel, Switzerland*

Received 7 December 1995; accepted 9 January 1996

Abstract--Five reaction stages have been identified in the reduction of pyracylene to its dianion. The same stages were also observed in the photochemical oxidation starting with the dianion. The formation of dimers of anions and of mixed valence aggregates is discussed.

The problem of packing several negative charges in a restricted space of a single, π-conjugated molecule is fundamental in the chemistry of novel carbanions. Recently, several polyanions were discussed vis á vis their electronic structure, magnetic properties, chemical reactivity, the effect of the counter cation and the unexpected formation of stable aggregates [1]. Diamagnetic polycyclic anions have been thoroughly studied by NMR spectroscopy [1]; and paramagnetic anions by EPR spectroscopy [2]. The formation of radical-trianions and factors governing their stability has been reported by Gerson [2].

The preparation of the carbanions of conjugated π-systems is being carried out via an electron transfer process by alkali metals leading to various degrees of charging, ranging from mono anions to hexa anions and even to more highly charged species [1-8].

$$A \xrightarrow{+e} A^{\bullet -} \xrightarrow{+e} A^{2-} \xrightarrow{+e} A^{3\bullet -} \xrightarrow{+e} A^{4-} \xrightarrow{+e} etc. \qquad (1)$$

In an alternating fashion some of these species have paired electrons and are diamagnetic, some have odd electrons and are paramagnetic. They can be studied by magnetic resonance spectroscopy [1,9], optical spectroscopy, X-ray diffraction (when crystallized) and undergo photo induced ET reactions in which solvated electrons are involved [10]. Very little is

known about the structure of non-planar conjugated anions, their aggregates and complexation with other anions. Reoxidation can also be performed by reverse photochemical processes, which eject electrons from polyanions.

$$A^{4-} \xrightarrow[h\nu]{+e} A^{3\bullet-} \xrightarrow[h\nu]{+e} A^{2-} \xrightarrow[h\nu]{+e} A^{\bullet-} \xrightarrow[h\nu]{+e} A \qquad (2)$$

However, the degree of charging depends on the π-conjugated skeleton. A recent observation and characterization of an exceptionally stable, high-order sandwich compound derived from the corannulene skeleton [1c,3] in which two delocalized hydrocarbon polyanions are held together by multiple lithium ions, both inside and out, has added a new feature to the landscape of organo-metallic chemistry [1c,d]. Derivatives of conjugated hydrocarbon dianions had previously been shown to exist preferentially as "ion triplets" with the lithium cations located on opposite faces of the dianion [7], and ion triplets with a single lithium ion between two organic anions had likewise been observed [8].

A combined structural study by NMR and EPR allows a detailed follow-up of the formation of such species. Chemical shifts and hyperfine splitting (hfs) in the EPR spectra are most informative.

Pyracylene radical anion, $Pyr^{\bullet-}$, and dianion, Pyr^{2-}, have been prepared by Trost *et al.*, [11a], however, their spectroscopic as well as structural properties were not fully established. The pyracylene molecule $C_{14}H_8$, Pyr, (Figure 1) represents a subunit of the C_{60} skeleton, and it also includes a fulvalene within its framework. Moreover, Pyr seems to be the single invariable unit of fullerenes in the course of their isomer conversion [11b]. These structural features make it and its anions worth a detailed examination. Also, like other condensed polycyclic molecules, Pyr poses a question about π-electrons delocalization mode [1,11c].

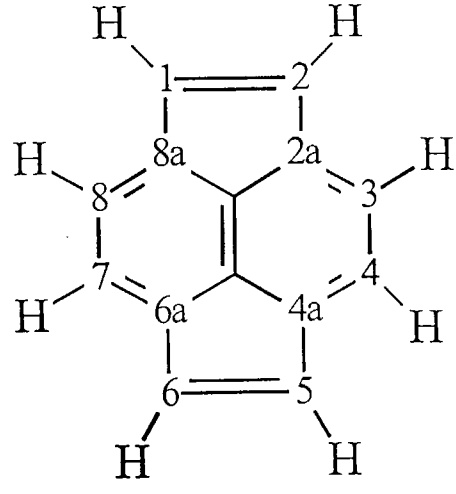

Figure 1. Molecular structure of pyracylene.

Pyr is easily reduced. So far, two polarographic half-wave reduction potentials (- 1.056 and -1.635 eV vs SCE) have been reported [11a], and the related EPR and NMR spectra of the radical anion and the dianion have been observed [11d,e]. It was proposed that in contrast to acenaphthylene dianion, in which the central carbon atom bears nearly a unit of charge [9], Pyr^{2-} would leave the two central atoms uncharged and behave as a [12] annulene with 14π electrons in the periphery. Trost *et al.* based their structure upon the excellent agreement of the ^1H NMR of $Pyr^{2-}/2Li^+$ with a model of a [12] annulene dianion, although ^{13}C NMR was not available [11d,e].

We report here our observations of a multi-step reduction process of Pyr in a combined uv-visible, NMR, and EPR spectroscopic study.

EXPERIMENTAL

Pyr was synthesized by FVP (flash vacuum pyrolysis) and purified chromatographically [11c]. THF (tetrahydrofuran, Aldrich Chemicals) was dried over Na/K alloy. Samples of Pyr/M/THF solutions were prepared under vacuum after a contact with the alkali-metal mirror (or wire for the case of Li). The experimental setup for the pulsed Fourier transform EPR (FT-EPR) measurements in the X-band region following pulsed laser excitation was described in detail previously [10]. Characterization of equilibrated spin systems was carried out by conventional CW-EPR detection with 100 kHz field modulation, by uv-visible absorption spectroscopy and by NMR (Bruker AMX-400, working at frequency of 400.13 MHz for ^1H). Quenching reactions were carried out in a polyethylene bag filled with argon. The sample tube was broken and the quenching reagent (D_2O or O_2) was added. Then the sample was checked by NMR.

RESULTS

Uv-visible Absorption Spectra

In contact with a potassium mirror the Pyr/THF solution passes through the reduction stages I-V, which are characterized by five different colors and consequently by five different uv-visible absorption spectra. Figure 2 shows such spectra for the potassium case. Similar phenomena have been observed for other alkali metals (Li, Na, Rb, Cs).

The *red* solution of neutral Pyr (Figure 2, I), after a short contact (a few seconds) with the potassium mirror, undergoes a color change to *bright orange*. This change has been ascribed to the formation of $Pyr^{\bullet-}$ (Figure 2, II) [11c]. Upon further reduction, a green color (species III, Figure 2) is observed. The next two stages are *yellow* (IV) and *dark green* (V) colored solutions. The transition times between stages III and IV and between IV and V are very short (seconds). Only by carefully monitoring the progress of the reduction and interrupting it after each color change was it possible to observe stages III and IV. This is, possibly, a reason for the earlier reports mentioning only three stages, i.e. I, II, and V. The understanding of the nature of the reduction stages III, IV and V is the

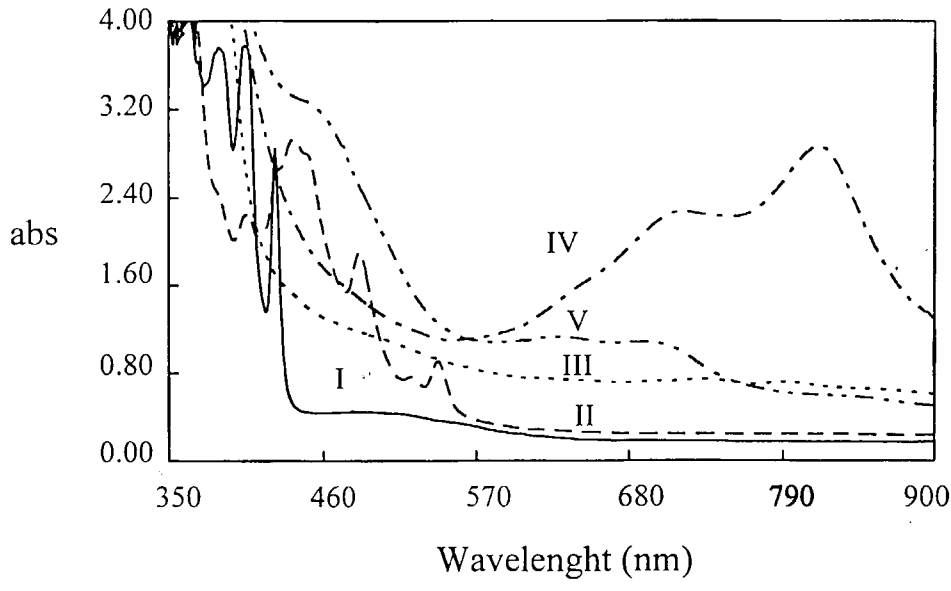

Figure 2. UV-vis spectra of all reduction stages of pyracylene; I - the neutral pyracylene; II - radical-anion; III - covalently linked dimeric dianion; IV - radical-anion dianion mixed dimer; V - dianion -dimer.

main goal of the present study. Obviously new species that differ from species I, II and V are presented. It should be noted, that spectra of stages III and V show some similarity and therefore, a similarity of the two species is expected. In order to identify the species of the various reduction stages, we have applied EPR and NMR spectroscopies.

EPR Spectra

Following the changes in the uv-visble spectra, each stage of reduction was recorded by EPR as follows:

1) The solution of the neutral Pyr, I, does not manifest any EPR signal.

2) The EPR spectrum of stage II in the Pyr/K system is shown in Figure 3a. The same spectrum for Pyr radical anion is obtained with Li, K, and Na and it is characterized by two sets, each one split by four equivalent protons, with the hyperfine splitting constants (hfsc's), a_1 = 1.94 and a_2 = 2.48 Gauss. This result is in full agreement with previous observations of $Pyr^{\bullet-}$ [11d]. This stage of the reduction with Rb and Cs is characterized by an EPR spectrum related to two sets of four equivalent protons (with a_1^{Rb} = 2.48, a_2^{Rb} = 1.94; a_1^{Cs} = 2.50 and a_2^{Cs} = 1.95 Gauss), and splitting by the alkali metal cation (with $a_M^{Rb(S=5/2)}$ = 0.545, $a_M^{Rb(S=3/2)}$ = 0.114 and $a_M^{Cs(S=7/2)}$ = 0.85 Gauss).

3) Stage III does not show any EPR signal.

4) Stage IV is characterized by a new EPR spectrum split by two sets of four equivalent protons and a set of hfsc due to *two* alkali-metal cations (see Figure 3b). The hfsc's for the different counterions are presented in Table 1.

5) The last reduction stage, i.e. V, does not manifest an EPR spectrum.

NMR Data

A detailed NMR study has been carried out for the Pyr/Li and Pyr/K systems.

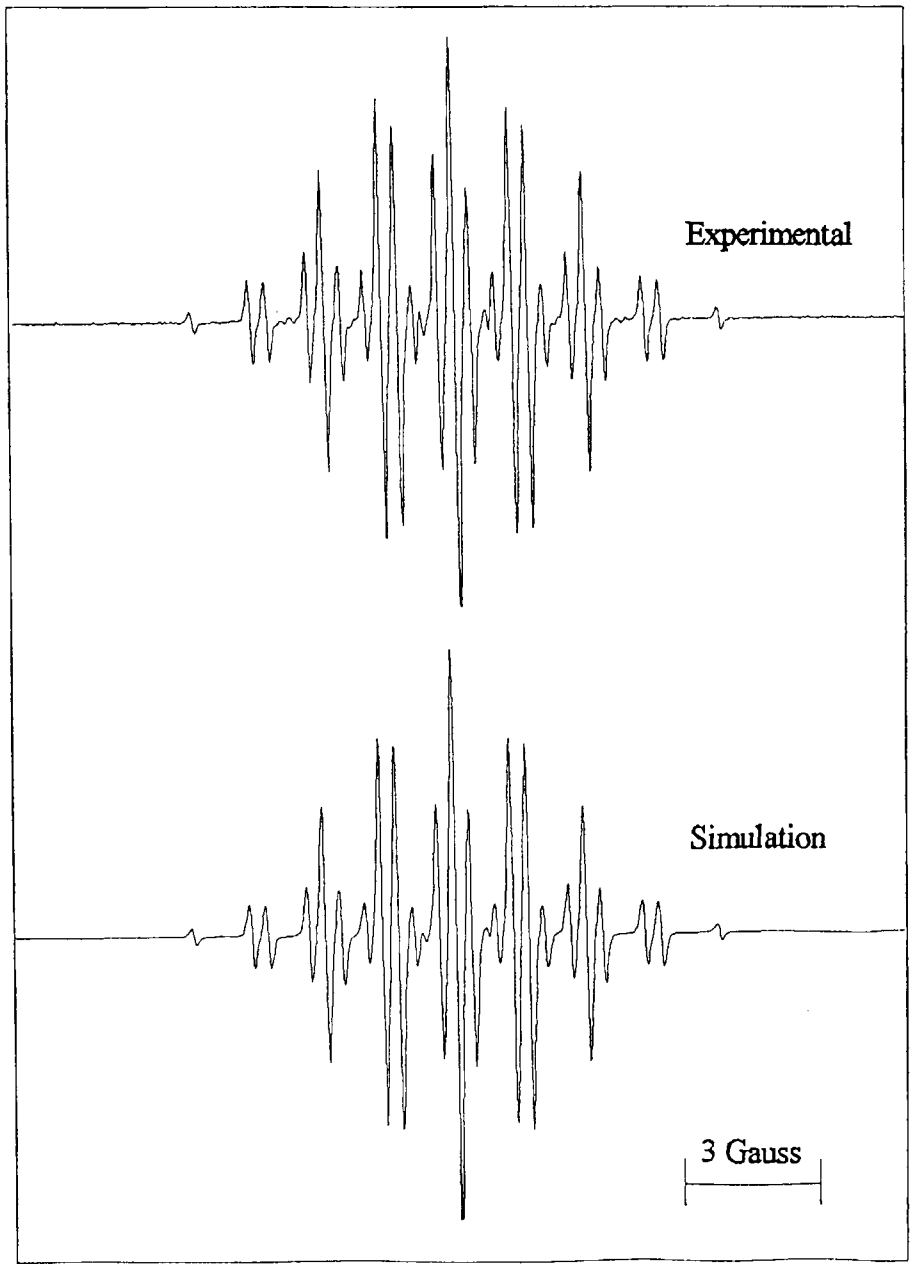

Figure 3a. Experimental and simulated CW EPR spectra of Pyr/K radical anion (stage II).

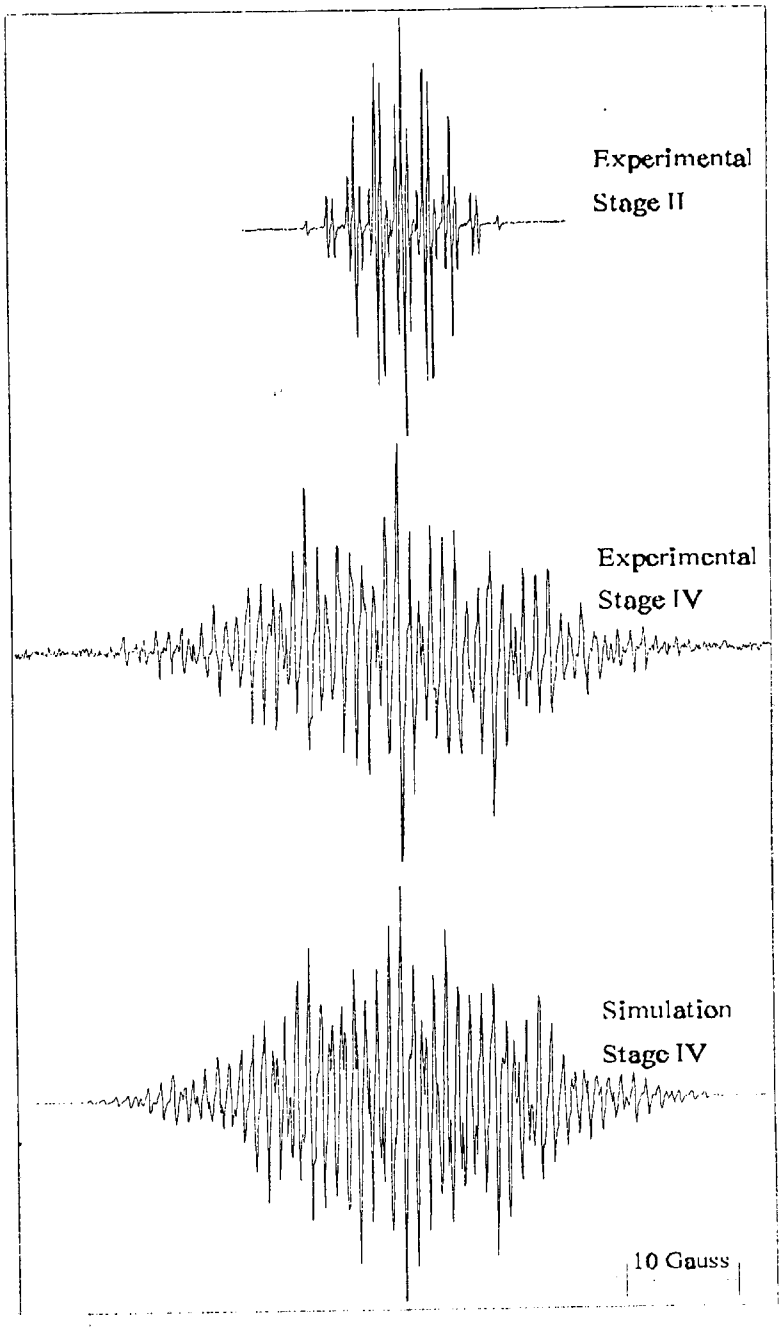

Figure 3b. Experimental and simulated CW EPR spectra of stage IV, note the difference between stage II (upper trace) and the experimental and simulated spectra of stage IV.

The ^{1}H NMR was used for the monitoring of all five reduction stages and the ^{13}C and ^{7}Li NMR spectroscopies for stage V only. Thus, we had an opportunity to find out the electron density on the particular carbon atoms and the total charge (^{1}H NMR and ^{13}C

Table 1

Hyperfine coupling constant for reduction stage IV of Pyr for different alkali-metals. Three hfs'c are observed: two groups for the protons (a_1 and a_2) and one group for the alkali metals (a_3).

Cation	a_1 (4H)	a_2 (4H)	a_3 (2M)
^{6}Li	4.17	8.54	1.16
^{7}Li	4.31	8.49	1.12
Na	4.06	8.47	0.96
K	4.17	8.64	1.16
Rb	4.17	8.61	1.16

NMR).

1) Stage I manifests an ^{1}H NMR spectrum with two sharp peaks at 6.19 and 6.71 ppm related to two unequivalent positions of the hydrogen atoms (Figure 1) in agreement with previous results (see Figure 4a) [11a].

2) Upon reduction, the above mentioned lines of the proton spectrum of Pyr starts to broaden, presumably due to an electron exchange process between Pyr and $Pyr^{\bullet-}$ (Figure 4b), and then completely disappears at stage II, where only the paramagnetic species ($Pyr^{\bullet-}$) is present.

3) A very broad single ^{1}H NMR line at 7 ppm with width of 0.5 ppm is observed for stage III (Figure 4c).

4) Stage IV does not manifest any NMR signals.

5) Stage V manifests a two-line ^{1}H NMR spectrum, 6.09 and 6.80 ppm (for Li cations) (Figure 4d) which differed only slightly from that of the neutral Pyr molecule and which has been previously observed in the last reduction stage and has been attributed to Pyr^{2-} [11d,e].

The ^{7}Li NMR spectrum shows a sharp single line at -7.2 ppm (Figure 5).

The ^{13}C NMR spectrum shows four lines (Table 2) related to four unequivalent positions of carbon atoms (Figure 1). Its center of gravity is shifted by 24.7 ppm as compared to the spectrum of the neutral Pyr molecule. For the assignment we used partially deuterated pyracylene, where most of the deuterium attached at position 1 and 5. The ^{13}C NMR tertiary peaks were assined by 2D ^{13}C - ^{1}H correlation experiments and the two quarternary ^{13}C peaks were assigned by their relative intensity (taking into account relaxation phenomena).

Quenching Experiments with Deuterium Oxide

To reveal the degree of charging of the species responsible for the NMR spectrum of stage V, deuteration with D_2O followed by NMR investigation of the formed product was carried out. The resulting ^{1}H NMR spectrum shows four equal-intensity lines: two doublets at 7.7

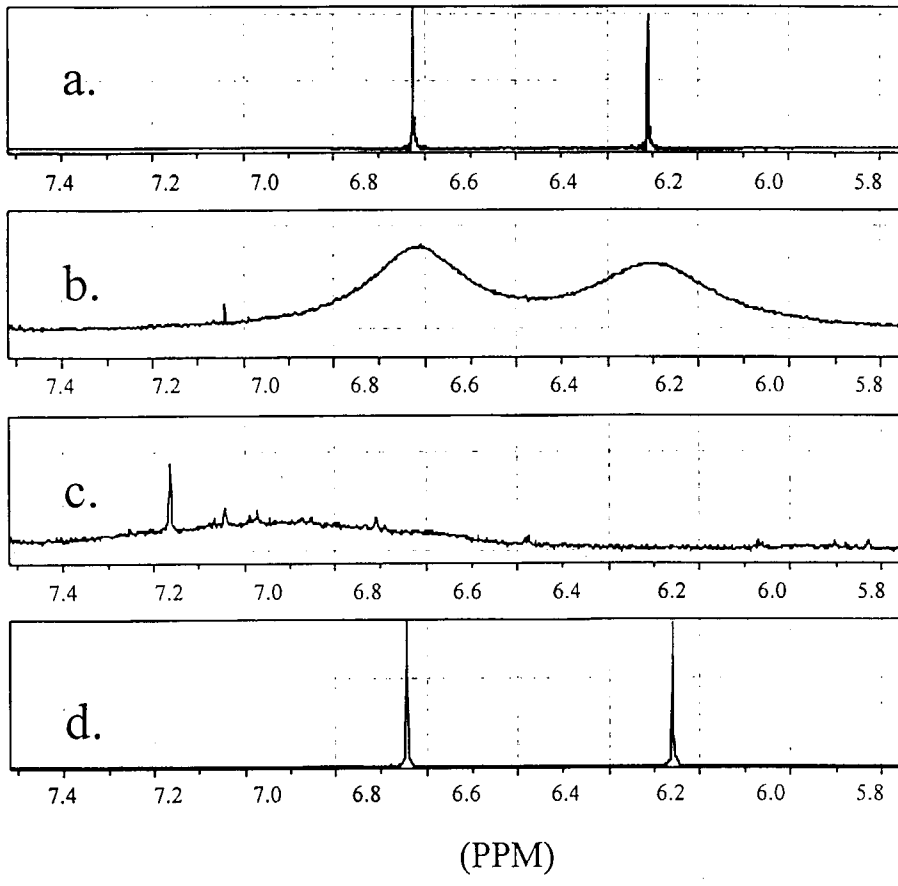

Figure 4. ^{1}H NMR spectra for different reduction stages. (a) neutral pyracylene (stage I); (b) line broadening upon transition to stage II; (c) ^{1}H NMR trace of stage III; (d) ^{1}H NMR bands of stage IV (pyracylene dianion).

and 7.35 ppm and two singlets at 7.05 and 3.55 ppm (Figure 6), thus showing that only two deuterium atoms are attached. Furthermore, the ^{13}C NMR spectrum of the product manifests coupling to deuterium of atoms C1 and C2 (or C5 and C6). These observations clearly show that the deuterated species is dideuteriopyracylene (Figure 7) and that the precursor is the dianion, Pyr^{2-}.

Photochemical Reoxidation

Irradiation of the fully reduced species with 532 nm laser light gives rise to the reverse reoxidation sequence:

$$V \xrightarrow{h\nu} IV \xrightarrow{h\nu} III \xrightarrow{h\nu} II \xrightarrow{h\nu} I \qquad (3)$$

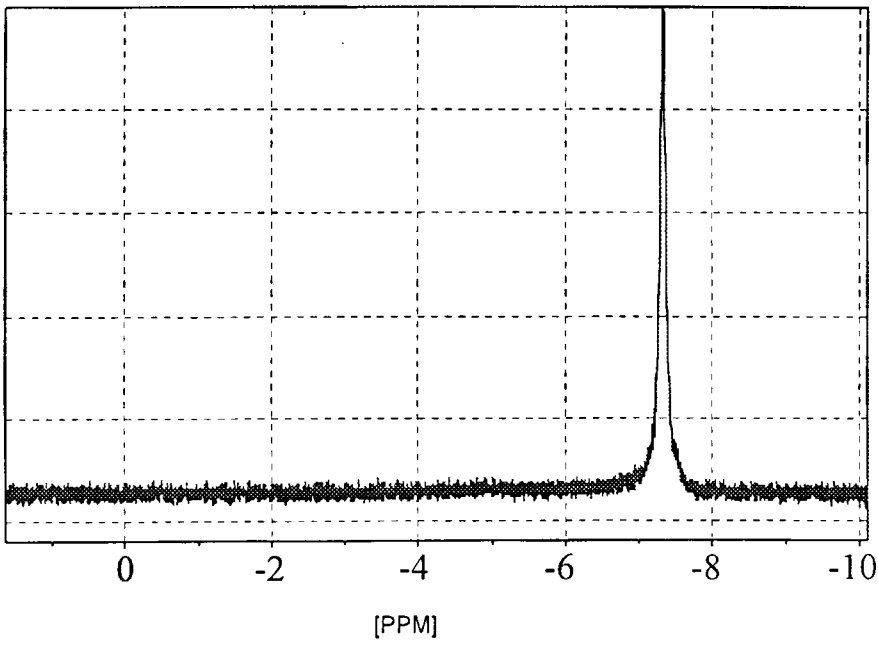

Figure 5. ^{7}Li NMR spectrum of stage V.

Table 2
^{13}C NMR chemical shift (ppm) of reduction stages I and V[a].

	C1,2,5,6	C3,4,7,8	C2a,4a,6a,8a	C2d,4b	center of gravity
Pyr(I)	133.6	125.9	143.4	133.0	134.1
$Pyr^{2-}/2Li^{+}$ (v)	94.3	111.0	113.7	**129.4**	109.6
$Pyr^{2-}/2Na$ (V)	95.5	111.7	110.8	**129.9**	109.4
$\Delta\delta_c$	-38.1	-14.2	-32.6	-3.1	-24.7
q_r	-0.2	-0.1	-0.2	0	

[a]In ppm relative to Tetramethylsilane.

With the exception of stage IV, the EPR spectra of the relevent stages are identical to the corresponding spectra observed upon direct metal reduction.

Oxidation of V → IV, shows, in addition to the EPR spectrum which is identical to the spectrum of the metal reduction stage IV, an additional line which is assigned to the photoejected electron [10,12].

Although the laser pulses were short and the FT EPR detection was sufficiently fast, all the spectra were in the absorptive mode and no specific electron spin polarization effects [12] were registrated.

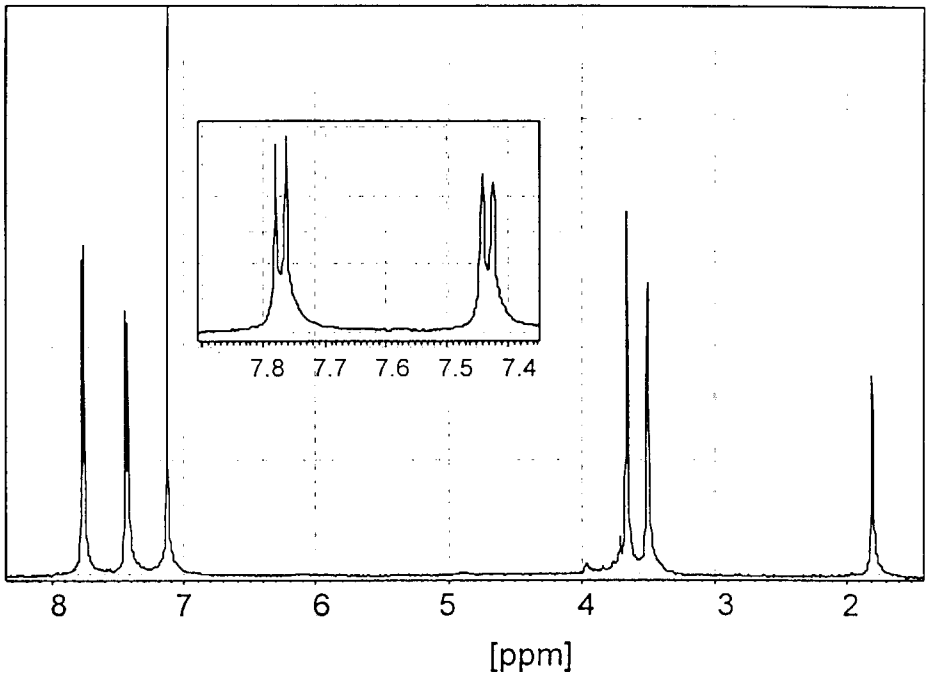

Figure 6. ^{1}H NMR spectrum of the quench product of the pyracylene dianion (stage V) with D_2O.

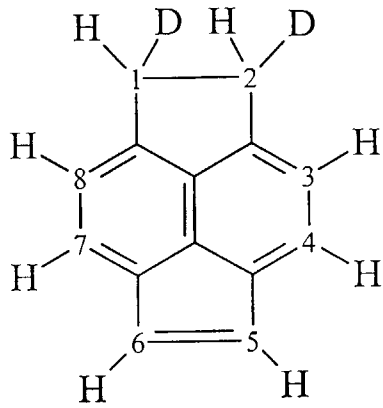

Figure 7. The structure of 1,2-dideuterio pyracylene.

DISCUSSION

Based on the above experimental results we suggest the following reduction mechanism occurring under the contact of Pyr(I) with alkali metal (Roman subindices point out the reduction stages):

$$Pyr_1 + M \rightarrow \{Pyr^{\bullet -}, M^{+}\}_{II} \quad (4)$$

$$\{Pyr^{\bullet -}, M^{+}\}_{II} + \{Pyr^{\bullet -}, M^{+}\}_{II} \rightarrow \{Ad^{2-}, 2M^{+}\}_{III} \quad (5)$$
$$Ad^{2-} = C_{28}H_{16}$$

where we assume that Ad^{2-} is a doubly charged covalent dimer with the structure shown in Figure 8a, thus the continuation of the reduction process leads to IV.

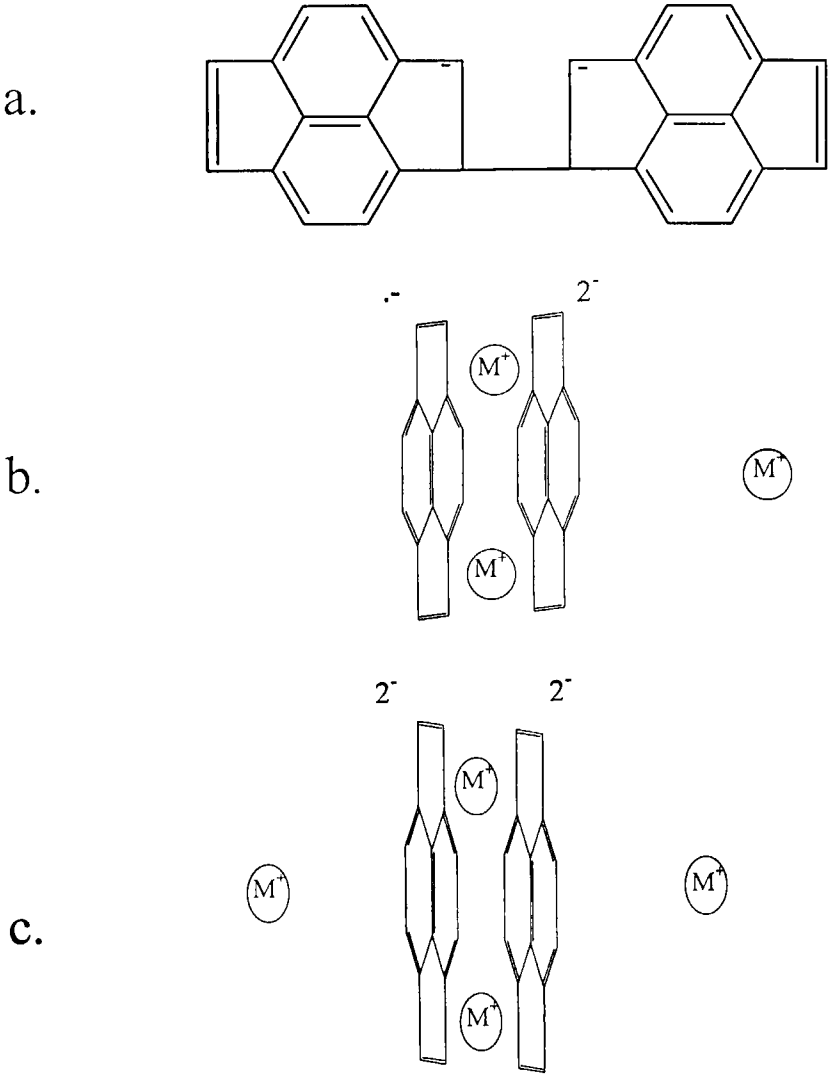

Figure 8. (a) Structure of the covalent dimer Ad^{2-}-(III); (b) The structure of the mixed dimer of radical anion-dianion IV; (c) The final reduction product V - a dianion dimer.

$$\{Ad^{2-}, 2M^{+}\}_{III} + M \rightarrow \{Pyr^{\bullet-}, 2M^{+}, Pyr^{2-}, M^{+}\}_{IV} \quad (6)$$

with the structure of IV shown in Figure 8b. The last step then follows:

$$(Pyr^{\bullet-}, 2M^{+}, Pyr^{2-}, M^{+})_{IV} + M \rightarrow \{M^{+}, Pyr^{2-}, 2M^{+}, Pyr^{2-}, M^{+}\}_{V} \quad (7)$$

with the structure of V shown in Figure 8c.

We suggest that both IV and V are formed via coulombic interactions with participation of three or four M^+ cations respectively, two of which are closely attached to the anions (contact ion pairs, CIPs) and the others are remote (solvent separated ion pairs, SSIPs).

The above mechanism meets all published and unpublished data, the most important points are listed below.

1) Five stages have been observed of different colors and different uv-visible absorption spectra. This points out to the existence of five different species.

2) The hf structure of the EPR spectra shows that species II is the radical anion, $Pyr^{\bullet-}$, coupled with a single counter-cation. Moreover, the larger cations (Rb^+ and Cs^+) form more tight ion pairs (and consequently they evoke larger hfsc's) as the smaller cations (Li^+, K^+ and Na^+) [13-15].

3) Species III is diamagnetic as is manifested by its NMR spectrum.

4) Species IV is paramagnetic. The hf structure of the EPR spectrum is in line with two adjoining countercations, reflecting the formation of CIP even for the small Li^+. CIP formation for some countercations is a typical situation of sandwich structures [3].

5) Species V is diamagnetic. Charge quenching points out that this species includes Pyr^{2-} in its structure. The Pyr^{2-} structure is also confirmed by the observed NMR spectrum which is similar to the NMR spectrum obtained for the deprotonation product of dihydropyracylene [11e].

6) The polarographic investigation discovers two reduction half-waves only [11a]. This limits the electron transfer to no more than two charges.

7) The photochemical reoxidation confirms a true redox character of the entire reaction chain.

Two issues are still left open: first, the big difference between hfsc's of $Pyr^{\bullet-}$ at the stage II and $Pyr^{\bullet-}$ at the stage IV, evoking a dramatic change in the EPR spectrum in the course of reduction (see Figure 3b and Table 1); second, an explanation of the single-line ^7Li NMR spectrum at stage V for the unequivalent positions of lithium into the suggested dimer complex.

To answer the first question we carried out HMO calculations. Figure 9a depicts the HMO energy diagram and eigenvector of the LUMO level of Pyr, which becomes occupied when $Pyr^{\bullet-}$ is formed. In stage II, the complex $\{Pyr^{\bullet-}, M^+\}$ represents SSIP (solvent separated ion pairs) and, thus, Hückel orbitals of Figure 9a do not have to be perturbed. In stage IV $Pyr^{\bullet-}$ and alkali-metal cations form CIP, and assume an increase of the Coulomb

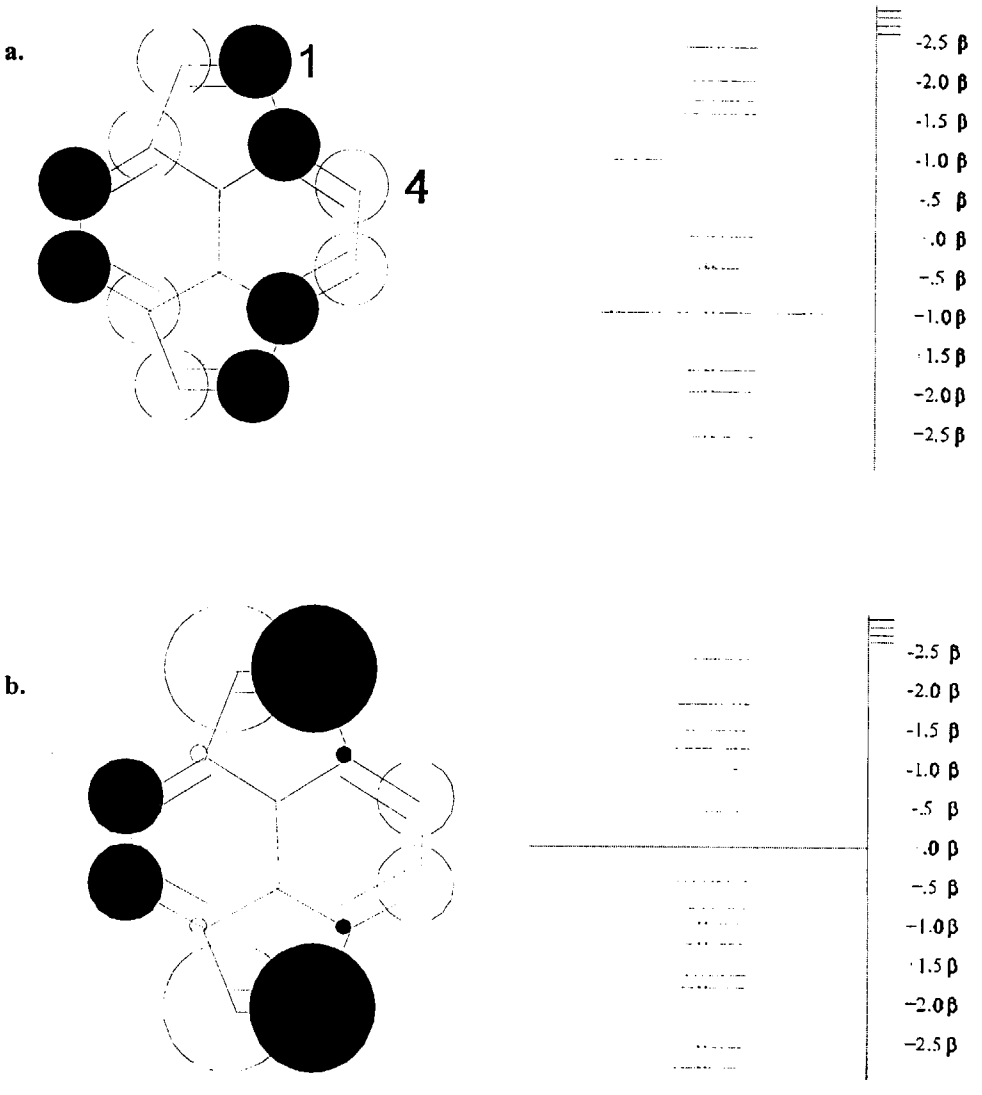

Figure 9. (a) HMO energy diagram and eigenvalues of the LUMO level of pyracylene; (b) HMO energy diagram and eigenvalues of the LUMO level of pyracylene - the Coulomb integral has been increased for C_1, C_2, C_5 and C_6.

integral. Computer simulation of such a situation (we increased Coulomb integral for C1, C2, C5 and C6) shows that the electron spin density on C1, C2, C5, C6 and C3, C4, C7, C8 is increased whereas the electron spin density on C2a, C4a, C6a, and C8a is decreased (Figure 9b). This substantiates an increase of the contact hfs interaction for two sets of equivalent carbons (C1, C2, C5, C6 and C3, C4, C7, C8) which is responsible for increasing the hfsc's (see Table 1). It is noteworthy that an increase of the Coulomb interaction for C3, C4, C7, and C8 evokes a drop of the electron spin density on both equivalent positions. Hence, this consideration undoubtedly points out that the cation is

located above the five-membered ring but not above the six-membered ring. Analogous results have been previously obtained for acenaphthylene [16].

A similar conclusion was obtained by more sophisticated, MNDO calculations [17,18], carried out for a complex of two Pyr^{2-} (species V). Moreover, the calculations show that alkali-metal cations are posed at the very edge of the five-membered ring, assuming a rapid exchange with the remote cations. This can be the reason for the observed single-line ^7Li NMR spectrum of species V. Similar results, namely polyanion-cation structures with some cations in a CIP state and the others in SSIP state, which exchange their location rapidly on the NMR time scale, have been previously obtained for a few multiply charged systems [1c,16,19]. Particularly, for the acenaphthylene dianion/$2Li^+$ structure one cation is in a CIP situation above the five-membered ring and the other solvated cation is more distant from the conjugated polycycle [16]. This is almost a direct analogy to the system under study because the acenaphthylene structure represents a considerable portion of the pyracylene skeleton.

Another explanation of the single-line ^7Li NMR spectrum can be the formation of an aggregate. In such a case, a statistically prevailing part of the cations have an identical chemical shift.

The self-association of ion pairs is not rare. For example, $\{(PhC{=}CPh)^{2-}, 2Na^+\}$ complexes form large aggregates in THF solution [20]. This is particularly noticeable for carbanions coupled with Li^+ cation [21].

The processes and species, involved in the Eqs. (4-7) require a few comments.

1) The chemical shift - charge density correlation [1,22-24], is a suitable method to deduce the π-charge distribution and aromaticity of species V. This method provides us with a linear dependence between the chemical shifts (δ) and the local π-charge measure on a particular carbon (q_π) [22-24]:

$$\Delta\delta = \delta_N - \delta_c = K_c\, q_\pi \qquad \textbf{(8)}$$

where δ_N and δ_c are the ^{13}C chemical shifts for the neutral and charged species correspondingly, and K_c is the proportionality factor. This method clearly shows that only a very small amount of the charge is located on the two central carbon atoms. Nearly all the extra π charge is dispersed over the periphery, in a fashion in which most of the charge is located on the fulvalenic moiety rather than on the naphthalenic one. More of that, the summation of these values over all carbons provides us with the full charge equal to two. The absence of charge at the hub and its dispersion over the perimeter confirms the description as a [12] annulene system with 14π electrons suggested by Trost *et al.*[11a]. Thus, an aromatic dianion is derived from an aromatic hydrocarbon.

2) The single-line ^7Li NMR spectrum of species V has been discussed above. Its negative position (-7.2 ppm) ensues from three factors: (a) the nature of the π-system, (b) the position of the lithium cation, and (c) the type of ion pairing. Sakurai *et al.* [25], showed (on the example of benzene dianion) that, for antiaromatic systems with cations located above a conjugated ring, the Li^+ cations are strongly deshielded by a paratropic ring

current of the π-electrons. In the Pyr^{2-} case, there is the opposite situation where the lithium cation in the same position is shielded by diatropic ring current that evokes the negative chemical shift, which was indeed observed. The magnitude of the ^7Li chemical shift must be determined by the extent of the ring-current interaction with the lithium cation, i.e., by the proximity of the cation to the anionic moiety. A very strong shielding has been observed for Li^+ of the aromatic cyclopenthadienyl lithium dissolved in DME (δ = -8.67 ppm); i.e. for system where the anion-cation pair exists as the CIP [26]. A considerable negative ^7Li NMR chemical shift in the Pyr/Li case probably, also relates to the existence of at least one CIP of pyracylene lithium salt.

3) Species III is a covalently linked diamagnetic dianion characterized by a broad ^1H NMR spectrum. It is formed in the reaction represented by Eq. (5) via the association of two radical anions. This reaction can proceed very fast in which C-C bonds are cleaved due to the influence of alkali metals, namely due to virtually reversible electron transfer from radical anion to cation and vice versa. In other words, electron transfer is associated with bond breaking and bond formation [27]. Similar reactions have been studied previously [28,29]. A good example [30] is the dimerization of 9-cyanoanthracene radical anions ($AnCN^{\bullet-}$) in aprotic solvents: $2AnCN^{\bullet-} \rightleftharpoons (AnCN)_2^{2-}$. The reversed dissociation reaction which should occur in the photochemical reoxidation sequence, probably also proceeds through the stage of photoinduced electron transfer inducing bond breaking.

CONCLUSION

Phenomena of multi-stage reduction are known for many systems [1,2]. A few examples are the nonalternant isopyrene [1,31,32] and corannulene [1c,3]. These systems show five reduction stages. Appearance of radical trianions and tetraanions has been corroborated by the EPR and NMR study. A very similar behavior was observed in this study for the case of Pyr/alkali-metal/THF systems. However, the latter system has completely different genesis. Although there is alternation of diatropic and paratropic stages, it ensues due to formation of the covalently linked dimer at stage III, and its reaction with the cation at stage IV. Herewith, the last species (stage V) consists of a pair of dianions complexed by four alkali-metal cations, $\{M^+, Pyr^{2-}, 2M^+, Pyr^{2-}, M^+\}$.

Acknowledgement

We thank Dr. Israel Shapiro for valuable discussions. We are grateful to Dr. David R. Duling, of the Laboratory of Molecular Biophysics, the National Institute of Environmental Science, National Institute of Health, USA, for using the EPR software. This work is in partial fulfillment of the requirements for a Ph.D. degree (G.Z.) at the Hebrew University of Jerusalem. Financial support by the US-Israel BSF grants (H.L.) and (M.R. and L.T.S.), the Israel Science Foundation (H.L., M.R. and V.R.), the Max Planck Research Award (H.L.), the Volkswagen Stiftung (H.L.), and the US National Science Foundation (L.T.S.) is gratefully acknowledged.

REFERENCES

1. a) M. Rabinovitz, *Topic Curr. Chem.* **146**, 99 (1988); b) M. Rabinovitz and R. Ayalon, *Pure App. Chem.* **65**, 111 (1993); c) A. Ayalon, A. Sygula, P.-Ch. Cheng, M. Rabinovitz, P.W. Rabideau, and L.T. Scott, *Science* **265**, 1065 (1994); d) M. Baumgarten, L. Ghergel, M. Wagner, A. Weitz, M. Rabinovtiz, P.Ch. Cheng, and L.T. Scott, *J. Am. Chem. Soc.* **117**, 6254 (1995) e) M. Baumgarten and K. Müllen, *Topics Curr. Chem.* **169**, 1 (1944); f) Y. Cohen, J. Klein, and M. Rabinovitz, *J. Am. Chem. Soc.* **110**, 4634 (1988).
2. F. Gerson and W. Huber, *Accounts Chemical Research* **20**, 85 (1987).
3. G. Zilber, V. Rozenshtein, P.-C. Cheng, L.T. Scott, M. Rabinovitz, and H. Levanon, *J. Am. Chem. Soc.* **117**, 10720 (1995).
4. a) J. Mortensen, H. Heinze, K. Herbst, and K. Müllen, *J. Electroanal. Chem.* **324**, 201 (1992); b) A. Bohner, H.-J. Räder, and K. Müllen, *Synth. Met.* **47**, 37 (1992).
5. K. Müllen, K.-W. alexander, F.-G. Klabunde, H.; Klärner, and T. Lund, *Chem. Ber.* **125**, 565 (1992).
6. A. Minsky, A.Y. Meyer, R. Poupko, and M. Rabinovitz, *J. Am. Chem. Soc.* **105**, 2164 (1983).
7. a) A. Streitwieser and T. Swanson, *J. Am. Chem. Soc.* **105**, 2502 (1983); b) A. Streitwieser, *Acc. Chem. Res.* **17**, 353 (1984).
8. a) M. Eiermann and K. Hafner, *J. Am. Chem. Soc.* **114**, 135 (1992); and references therein; b) G. Fraenkel and M.P. Hallden-Abberton, *J. Am. Chem. Soc.* **103**, 5657 (1981).
9. A. Minsky, A.Y. Meyer, K. Hafner, and M. Rabinovitz, *J. Am. Chem. Soc.* **105**, 3975 (1975).
10. a) V. Rozenshtein, G. Zilber, M. Rabinovitz, and H. Levanon, *J. Am. Chem. Soc.* **115**, 5193 (1993) b) G. Zilber, V. Rozenshtein, H. Levanon, and M. Rabinovitz, *Chem. Phys. Lett.* **196**, 255 (1992).
11. a) B.M. Trost, *Topics in Nonbenzenoid Aromatic Chemistry*, Hirokawa Publ. Co., Tokyo, 1973; Vol. I, p. 243; b) D. Babic and N. Trinajstic, *Comp. Chem.* **17**, 271 (1993) c) B. Freiermuth, S. Gerber, A. Riesen, J. Wirz, and M. Zehnder, *J. Am. Chem. Soc.* **112**, 738 (1990); d) B.M. Trost, S.F. Nelsen, and D.R. Britelli, *Tetrahedron Lett.* **40**, 3959 (1967) e) B.M. Trost, D. Buhner, and G.M. Bright, *Tetrahedron Lett.* **29**, 2787 (1973).
12. V. Rozenshtein, G. Zilber, and H. Levanon, *J. Phys. Chem.* **98**, 4236 (1994).
13. Y. Marcus (Ed.), *Ion Solvation*, Wiley, New York, 1985.
14. T.E. Hogen-Esch and J. Smid, *J. Am. Chem. Soc.* **88**, 307 (1966).
15. T.E. Hogen-Esch, *Adv. Phys. Org. Chem.* **15**, 153 (1977).
16. B. Eliasson and U.J. Edlund, *Chem. Soc. Perkin Trans. II* 1837 (1983).
17. M.J.S. Dewar and W. Thiel, *J. Am. Chem. Soc.* **99**, 4899 (1977).
18. W. Thiel, *QCPE* **2(438)**, 63 (1982).
19. G. Levin, B. Lundgren, M. Mohammad, and M. Szwarc, *J. Am. Chem. Soc.* **97**, 262 (1975).
20. G. Levin, J. Jagur-Grodzinski, and M. Szwarc, *J. Am. Chem. Soc.* **92**, 2268 (1970).
21. M. Szwarc (Ed.), *Ions and Ions Pairs in Organic Reactions*, Wiley, New York, 1972, Vol. 1, p. 1.
22. G.K. Fraenkel, R.E. Carter, A.D. McLauchlan, and J.H. Richrdson, *J. Am. Chem. Soc.* **82**, 5846 (1960).
23. T. Schaefer and W.G. Schneider, *Can. J. Chem.* **41**, 966 (1963).
24. B. Eliasson, U. Edlund, and K. Müllen, *J. Chem. Soc. Perkin Trans II.* 937 (1986).
25. A. Sekiguchi, K. Ebate, C. Kabuto, and H. Sakurai, *J. Am. Chem. Soc.* **113**, 7081 (1992).
26. R.H. Cox and H.W. Terry, *J. Magn. Reson.* **14**, 317 (1974).
27. J.M. Saveant, *Accounts Chemical Research* **26**, 455 (1993).
28. A. Lagendijk and M. Szwarc, *J. Am. Chem. Soc.* **93**, 5359 (1971).
29. T.D. Walsh, *J. Am. Chem. Soc.* **109**, 1511 (1987)..
30. R. Eliason, O. Hammerich, and V.D. Parker, *Acta Chem. Scan.* **B42**, 7 (1988).
31. B.C. Becker, W. Huber, and K. Müllen, *J. Am. Chem. Soc.* **102**, 7803 (1980).
32. W. Huber, *Helv. Chim. Acta* **66**, 2582 (1983).